Supplemental Table 1

Supplemental Table 1. AtSLP2-specific protein interactors recovered from cell culture and root tissue.

Cell Culture Pull-Downs																Root Pull-Downs					Rosette Pull-Downs					
Gene Name	Locus Tag	GFP_CTAP_control_1	GFP_CTAP_control_2	GFP_CTAP_control_3	GFP_CTAP_control_4	GFP_CTAP_control_5	GFP_CTAP_control_6	AtSLP2_cTAPa_1	AtSLP2_cTAPa_2	AtSLP2_cTAPa_3	AtSLP2_cTAPa_4	AtSLP1_cTAPa_1	AtSLP1_cTAPa_2	AtSLP1_cTAPa_3	AtSLP1_cTAPa_4	AtSLP2_cTAPa_1	AtSLP2_cTAPa_2	AtSLP1_cTAPa_1	AtSLP1_cTAPa_2	AtSLP1_cTAPa_3	AtSLP1_cTAPa_1	AtSLP1_cTAPa_2	AtSLP1_cTAPa_3	AtSLP1_cTAPa_4	AtSLP2_cTAPa_1	AtSLP2_cTAPa_2
AT1G18480	**AT1G18480**							15	131	89	180					5	25								7	21
HSP60-3A	**AT3G13860**							7		5	2					4	14						1			5
AtMIA40	**AT5G23395**							5	7	2	30					2	2								1	2
AT1G72730	**AT1G72730**															3	3		6					1	2	2
GSR 1	**AT5G37600**															3	2			10						2

Each interactor was identified via TAP pull-downs. Specificity of the interaction with AtSLP2 was determined relative to control pull-downs involving GFP-TAP or AtSLP1-TAP constructs. Total peptide number identified in each pull-down is presented.

Supplemental Table 2

Supplemental Table 2. Phosphorylated peptide substrates used in AtSLP2 assays.

Name	Phosphorylated Amino Acid	Sequence
RRP1B	pThr	SSKKV**T***FGLN
BRCA1	pThr	QSPKV**T***FECEQK
Ki67	pSer	KRRRV**S***FGGH
B56	pSer	KRAEEFLTA**S***QELAL
p38beta	pThr / pTyr	EEM**T***G**Y***VATR
p38	pThr / pTyr	EM**T***G**Y***VVTC
Rat SAPK3	pTyr	RQADSEMTG**Y***VVTR
hSAPK4	pTyr	RHADAEMTG**Y***VVTR

Starred and bold amino acids denote phosphorylated residues.

Supplemental Table 3

Supplemental Table 3. Primers for qPCR analysis of GA-related genes.

Gene	Primer Name	Primer Sequence
At1g18480	SLP2qLP	5'-ATCTTCCTGCCCCAAGATCC-3'
	SLP2 qRP	5'-CCATCTGTCCGACGAATCAA-3'
At5g25900	GA3 qLP	5'-ACTTCTTGATGTCGGAAGCG-3'
	GA3 qRP	5'-TTGCACAGACGATCTTGGAC-3'
At3g05120	GID1A qLP	5'-TCTACGATACTCTTTGTCGC-3'
	GID1A qRP	5'-TTAAAGCCACATTATGCGCG-3'
At3g03450	RGL2 qLP	5'-TCAAGCTGGAGCTATGGGAA-3'
	RGL2 qRP	5'-AGTGCATCTCCAAAACCTCT-3'
At1g14920	RGA1 qLP	5'-GCGATCGATAAGGTTCTTGG-3'
	RGA1 qRP:	5'-AAACCTCCGACATGACCTTG-3'
At5g23395	MIA40 qLP	5'-AGGGATCAGACTGCGTGAATC-3'
	MIA40 qRP	5'-AGGAGGCTGCTCTTCCTTTTTC-3'
At1g13440	REF qLP	5'-TTGGTGACAACAGGTCAAGCA-3'
	REF qRP	5'-AAACTTGTCGCTCAATGCAATC-3'

Supplemental Figure S1

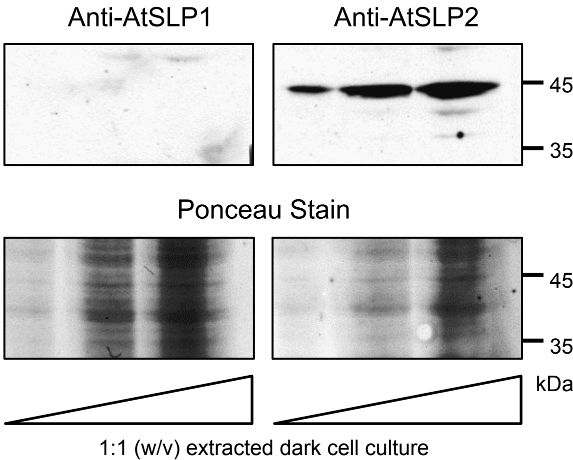

Supplemental Figure S1. Immunoblot analysis of dark-grown, wild-type *A. thaliana* cell culture. Cell culture extracted 1:1 (w/v) in 1x SDS-PAGE sample buffer was run in increasing volumes of 5, 15 and 30 µl on SDS-PAGE, transferred to a membrane and probed with affinity-purified anti-AtSLP1 and anti-AtSLP2 IgG (Uhrig and Moorhead, 2011) at 1.5 and 1.2 µg/mL, respectively.

Supplemental Figure S2

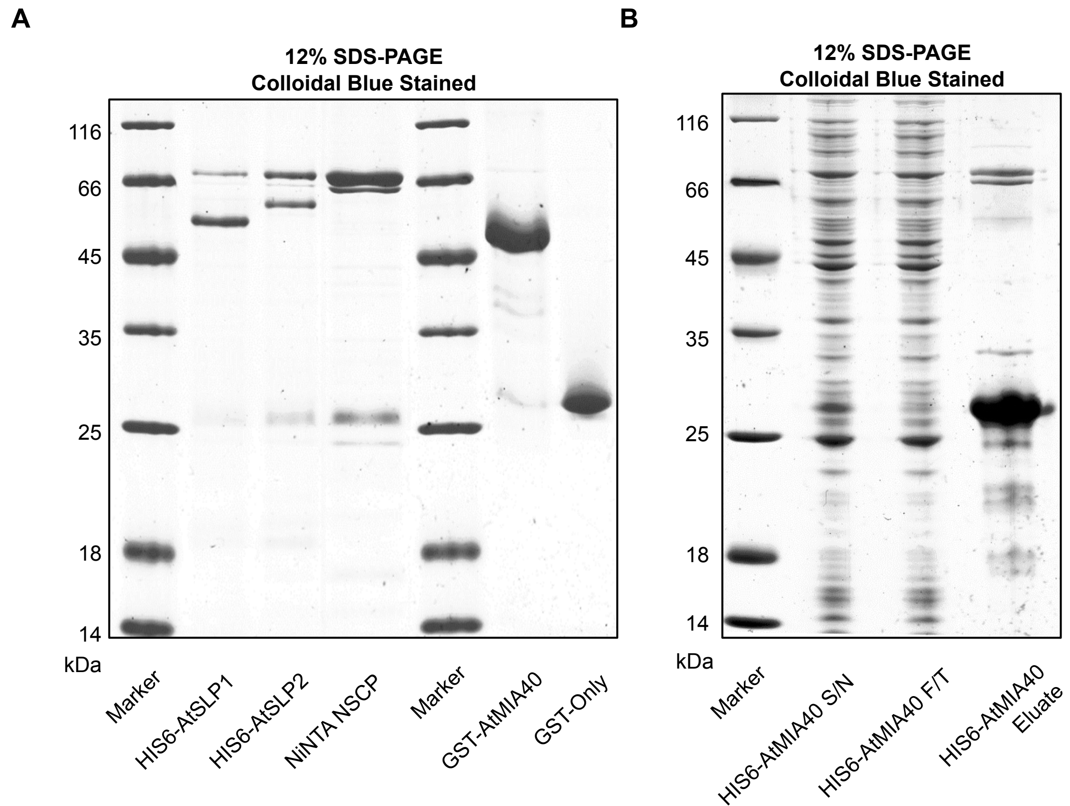

Supplemental Figure S2. Colloidal blue-stained purified fractions of bacterially expressed and purified *A. thaliana* proteins used during *in vitro* experimentation. A, Purified fractions of HIS6-tagged AtSLP1, AtSLP2 and non-specific co-purifying proteins (NCSP) as well as GST-tagged AtMIA40 and GST-only. B, Purified HIS6-tagged AtMIA40 eluate along with clarified HIS6-AtMIA40-expressing bacterial cell supernatant (S/N) and Ni-NTA flow-through (F/T). Each lane was loaded with 5 µg of total protein. Expression and purification conditions are presented in Methods section.

Supplemental Figure S3

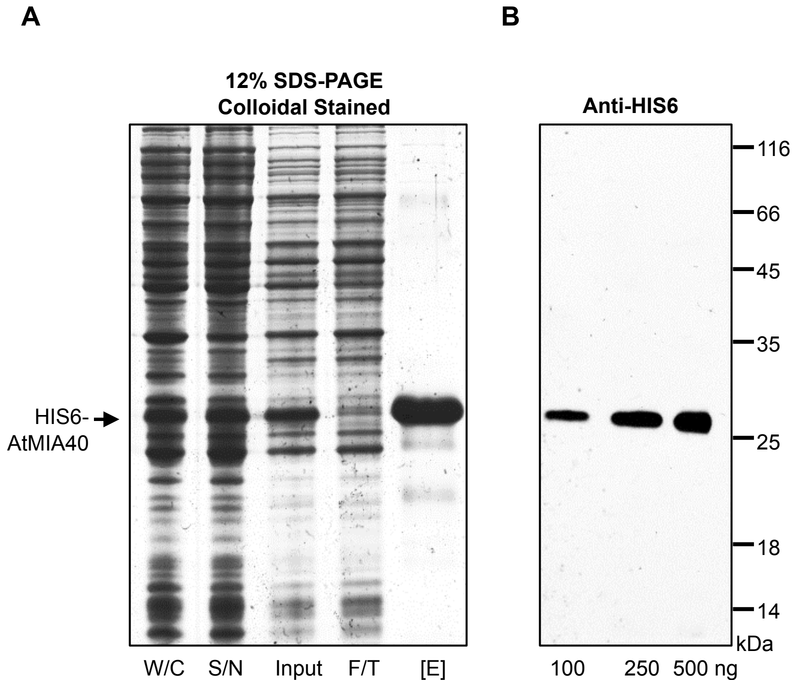

Supplemental Figure S3. Purification of 6 M urea extracted HIS6-AtMIA40. A, Purification scheme for 6 M urea extracted HIS6-AtMIA40. Whole cell (W/C), clarified supernatant (S/N), 6 M urea extracted protein pellet loaded on Ni-NTA (input), Ni-NTA flow-through (F/T) and concentrated Ni-NTA Eluate ([E]) are depicted. B, Dilution series of purified, 6 M urea-extracted HIS6-tagged AtMIA40 [E] subjected to immunoblot analysis using anti-HIS6 IgG. Each lane of the Colloidal stained gel contains 5 μg of total protein.

Supplemental Figure S4

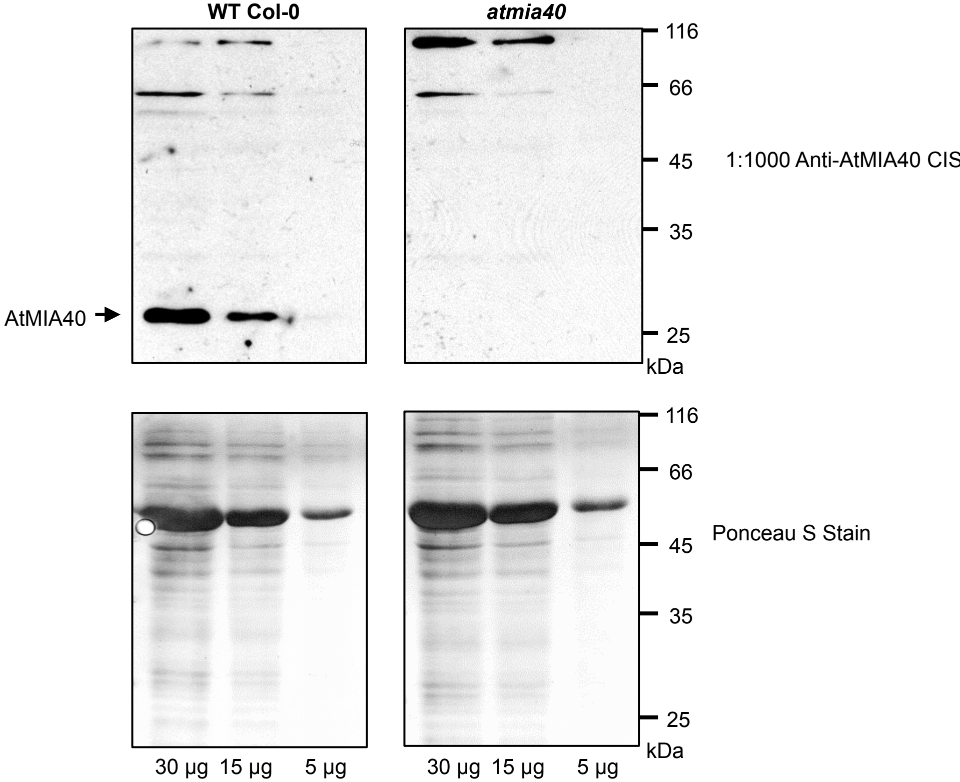

Supplemental Figure S4. Analysis of anti-AtMIA40 crude immune serum. Wild-type *A. thaliana* Col-0 (WT Col-0) and insertional *atmia40* knockout (*atmia40)* roots were employed to assess the detection of endogenous AtMIA40 by anti-MIA40 crude immune serum (CIS). Samples from WT Col-0 and *atmia40* were run on SDS-PAGE, transferred to a membrane and first stained with Ponceau S to show equal loading, then probed with 1000-fold diluted crude immune serum. The total protein of each lane is shown.

Supplemental Figure S5

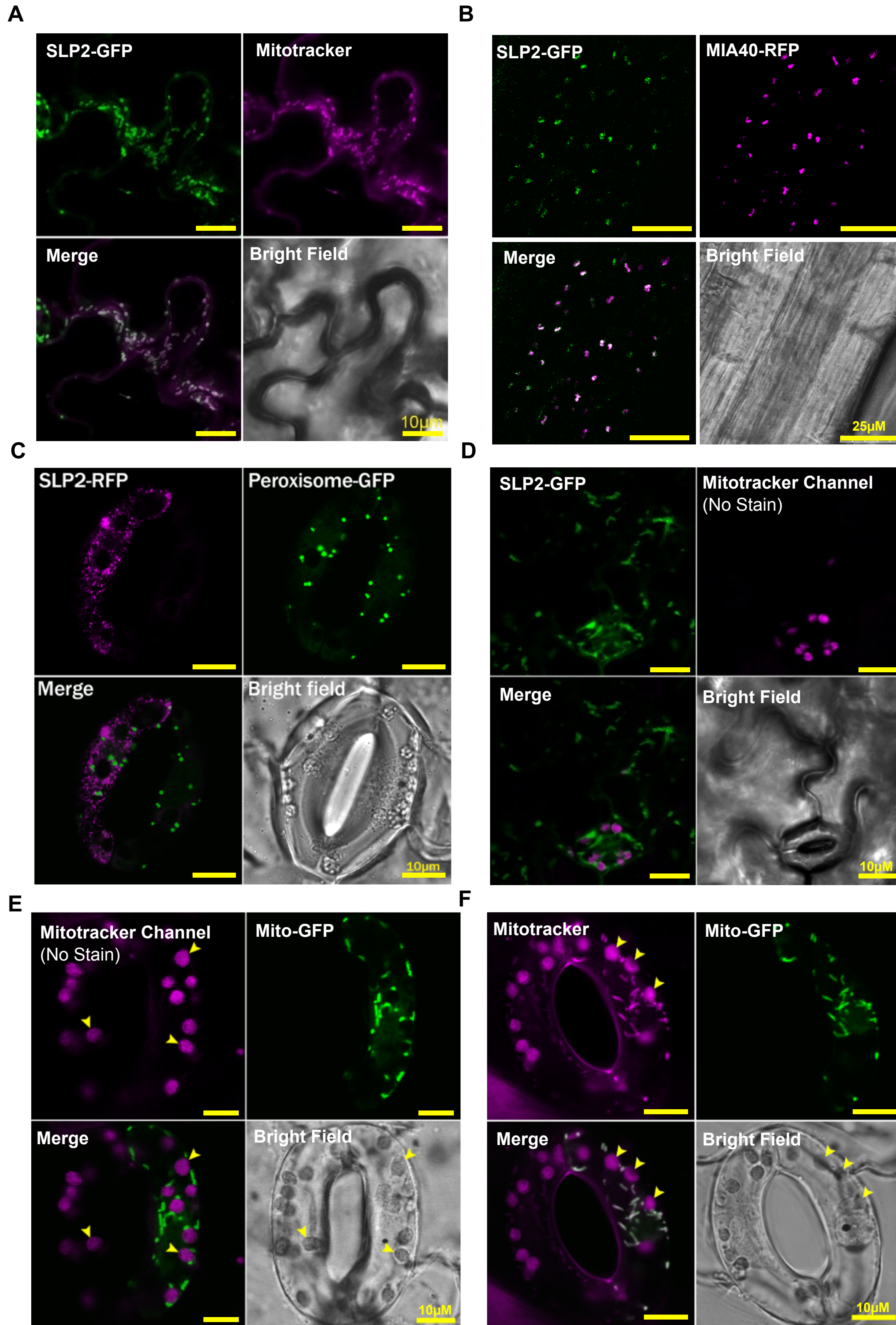

Supplemental Figure S5. Confocal imaging of AtSLP2 and AtMIA40 in plant cells. A, Pavement cells from *$35S_{pro}$::AtSLP2-GFP A. thaliana* plants co-localized with FarRed MitoTracker. B, Root cells from *$35S_{pro}$::AtSLP2-GFP/$35S_{pro}$:AtMIA40-RFP A. thaliana* plants. C, *Vicia faba* stomatal cells from *$35S_{pro}$::AtSLP2-RFP* plants imaged with peroxisome-targeted GFP. D, *A. thaliana* leaf cells from *$35S_{pro}$::AtSLP2-GFP* plants and the MitoTracker channel (no stain) reveal chloroplast autofluorescence. E, *Vicia faba* stomata transiently expressing mitochondrially targeted GFP. F, *Vicia faba* stomata transiently expressing mitochondrially targeted GFP and stained with MitoTracker. Yellow arrows (E and F) depict chloroplasts and their corresponding autofluorescence emitting at the same wavelength of the FarRed MitoTracker stain.

Supplemental Figure S6

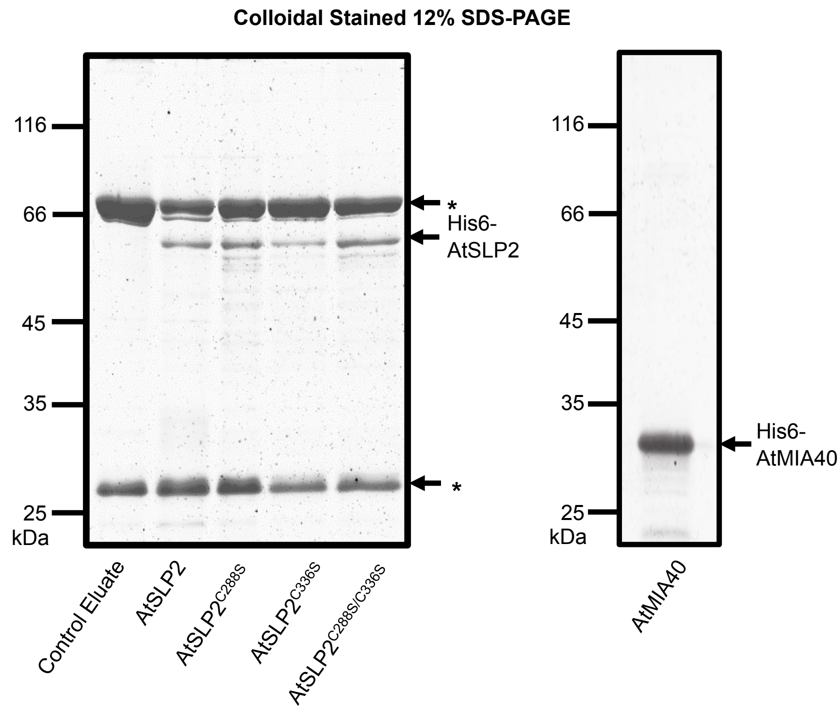

Supplemental Figure S6. SDS-PAGE analysis of purified HIS6-AtSLP2 and AtMIA40. Colloidal stained HIS6-AtSLP2 and HIS6-AtSLP2 cysteine site-directed mutants used in AtSLP2 phosphatase activity assays. From left to right, a control eluate, wild-type AtSLP2, AtSLP2^{C288S}, AtSLP2^{C336S} and double mutant AtSLP2$^{C288S/C336S}$. The weak expressing SLP2 band of and its variants are indicated. Left panel contains 10 µg of HIS6-AtSLP2 Ni-NTA eluate, while the right panel depicts 10 µg of HIS6-AtMIA40 Ni-NTA eluate. AtSLP2 constitutes approximately 10% of total protein in each extract. Stars (*) denote non-specific co-purifying proteins.

Supplemental Figure S7

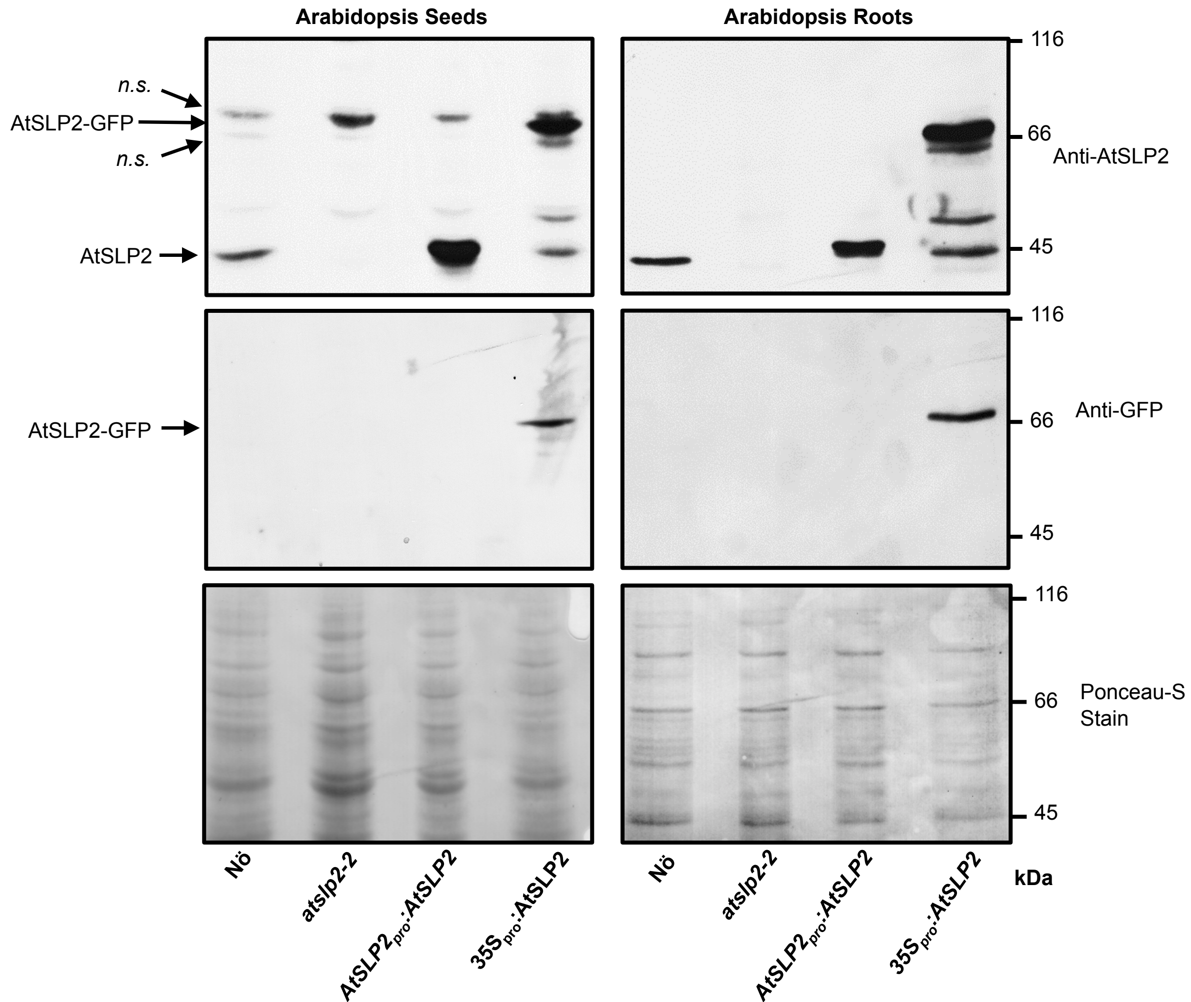

Supplemental Figure S7. Immunoblot analysis of *atslp2-2*, WT NÖ, *AtSLP2$_{pro}$:AtSLP2* complemented *atslp2-2* and *35S$_{pro}$:AtSLP2 A. thaliana* seed and root tissue. As AtSLP2 protein is only observed in seed and root tissue (Uhrig and Moorhead, 2011), western blotting of these tissues from the plant lines employed in this study was conducted. Western blots were probed with 1.5 µg/mL affinity-purified rabbit anti-AtSLP2 IgG (Uhrig and Moorhead, 2011) and 1:1000 mouse anti-GFP IgG (Roche, #11814460001). Endogenous AtSLP2 can be seen at ~45 kDa, while *35S$_{pro}$::AtSLP2* (GFP-AtSLP2) can be seen at ~68 kDa. Neither protein was detected in *atslp2-2* seeds and roots. Non-specific protein detection can be observed in seed samples and is denoted by *n.s*. Each lane contains 10 µg of total protein.

Supplemental Figure S8

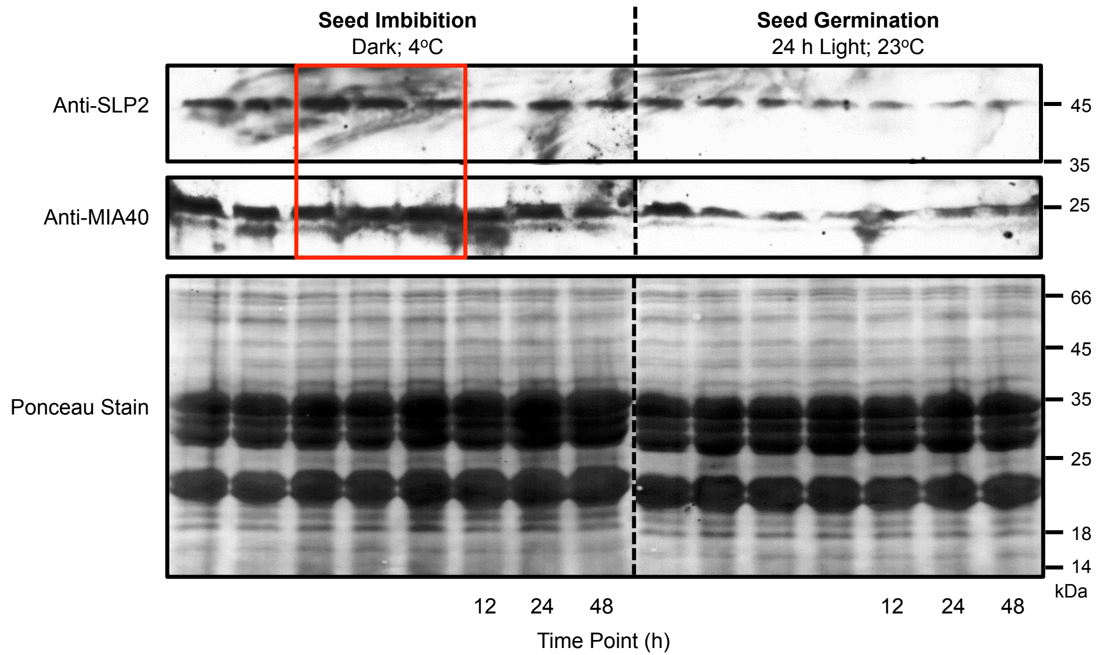

Supplemental Figure S8. Western blot analysis of AtSLP2 and AtMIA40 expression in imbibed and germinating seeds. Wild-type NÖ seeds were imbibed at 4ºC for the given time prior to extraction. Time course samples were run on SDS-PAGE, transferred to a membrane and first stained with Ponceau S to show equal loading, then probed with 1.2 µg/mL affinity purified anti-AtSLP2 antibody (Uhrig and Moorhead, 2011) or 500-fold diluted anti-AtMIA40 crude immune serum. Both AtSLP2 and AtMIA40 are most abundant early in seed germination. Each lane contains 30 µg of total protein. Red box depicts peak AtSLP2 protein levels.

Supplemental Figure S9

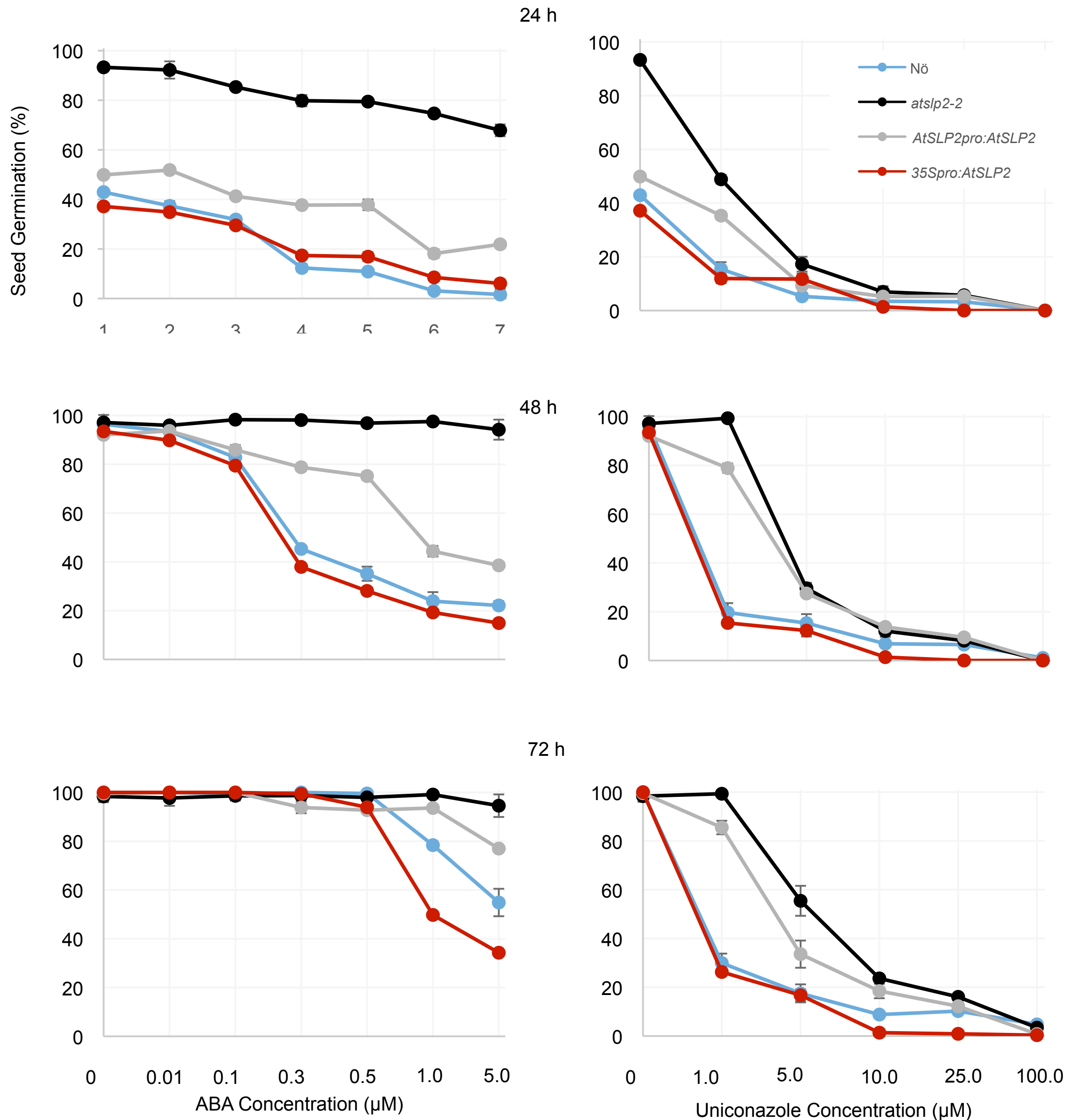

Supplemental Figure S9. Quantitative time-course measurement of seed germination on 0.5 x MS-agar plates containing ABA or Uniconazole. Control plates consisted of 0.5 x MS only. WT NÖ (blue), *atslp2-2* (black), $AtSLP2_{pro}$*::AtSLP2* (grey) and $35S_{pro}$*::AtSLP2* (red) are depicted. All seeds were imbibed at 4ºC for 48 h on each plate prior to germination under 16 h light : 8 h dark at 23ºC. Error bars represent ± standard error (n=3 plates of 80-120 seeds each).

Supplemental Figure S10

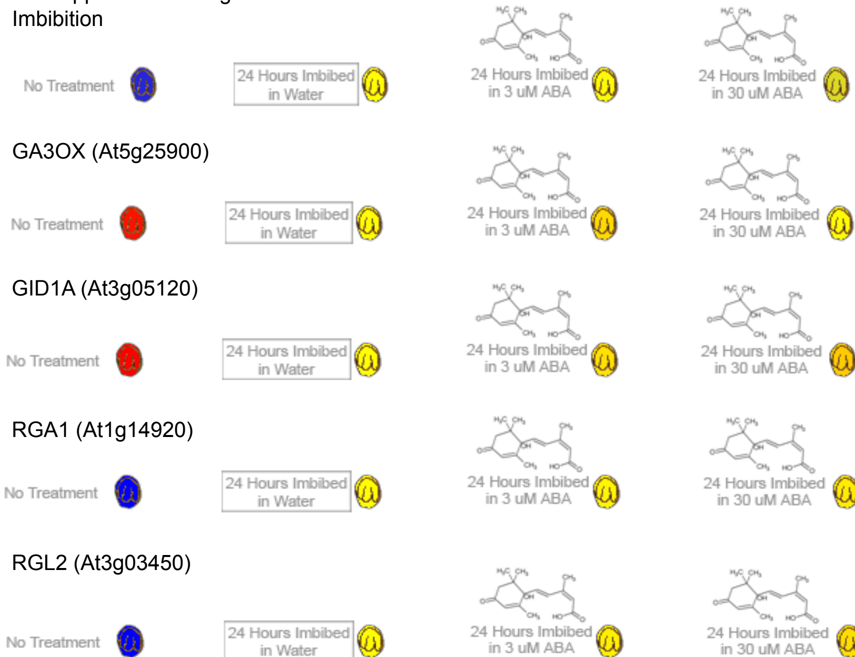

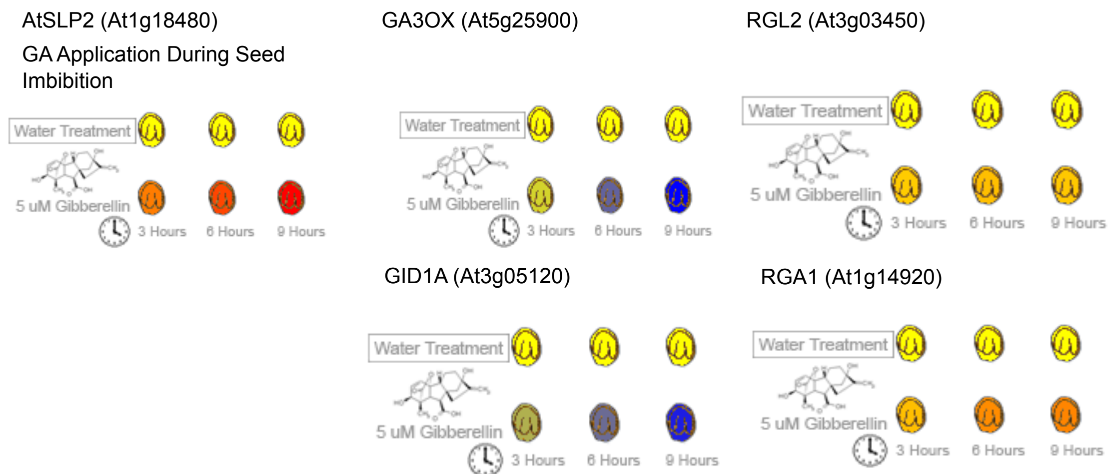

Supplemental Figure S10. Relative transcriptional expression of GA-related biosynthetic and signaling proteins from Biological Arabidopsis Resource (BAR). A, Changes in post-imbibition (48 h) GA-related gene expression in response to the presence of ABA. B, Changes in post-imbibition (48 h) GA-related gene expression in response to seed imbibition in the presence of GA. Gene identifiers (i.e. *AtSLP2; At1g18480*) are shown. Yellow represents no change, while different shades of red and blue represent a relative increase and decrease in transcript expression, respectively. All data were obtained from microarray experiments compiled at BAR (http://bar.utoronto.ca/).

Supplemental Figure S11

A

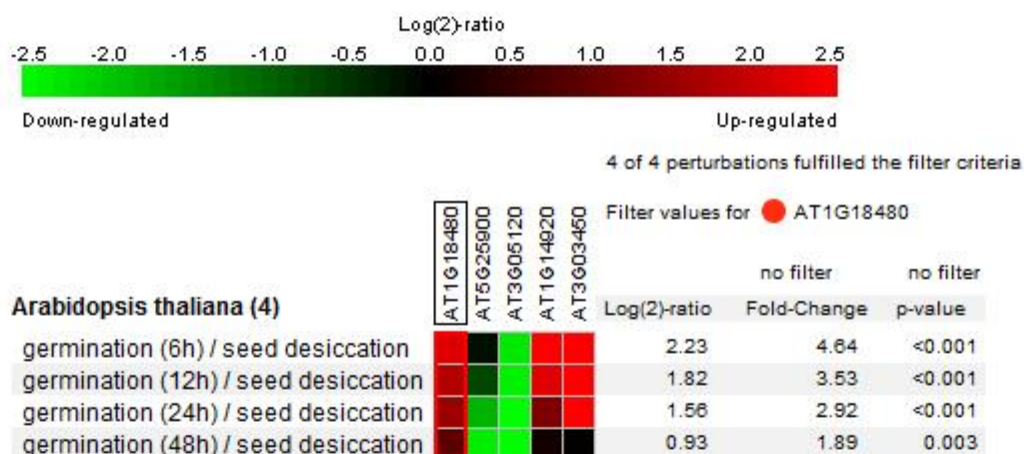

B

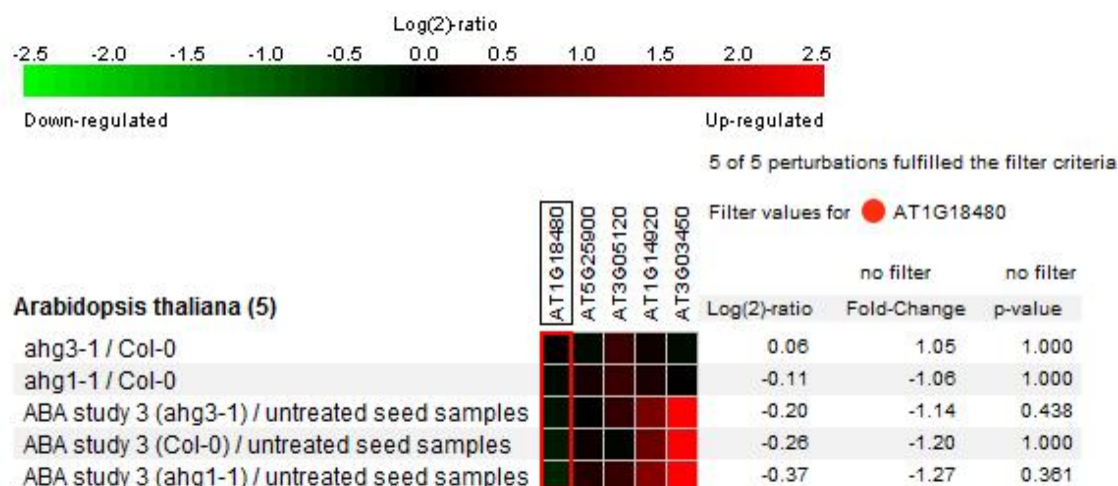

Supplemental Figure S11. Relative transcriptional changes in GA-related biosynthetic and signaling proteins as well as AtSLP2 from Genevestigator*.* A, Changes in post-imbibition (48 h) GA-related gene expression over a 48 h germination time-course of wild-type *A.thaliana* Col-0. B, Changes in post-imbibition (48 h) GA-related gene expression in response to the presence of 0.5 µM ABA using both Col-0 and two ABA HYPERSENSITIVE GERMINATION (*ahg*) mutant plant lines. Gene identifiers (i.e. *AtSLP2; At1g18480*) are shown. All data was obtained from microarray data compiled at Genevestigator (https://genevestigator.com/gv/).

Supplemental Figure S12

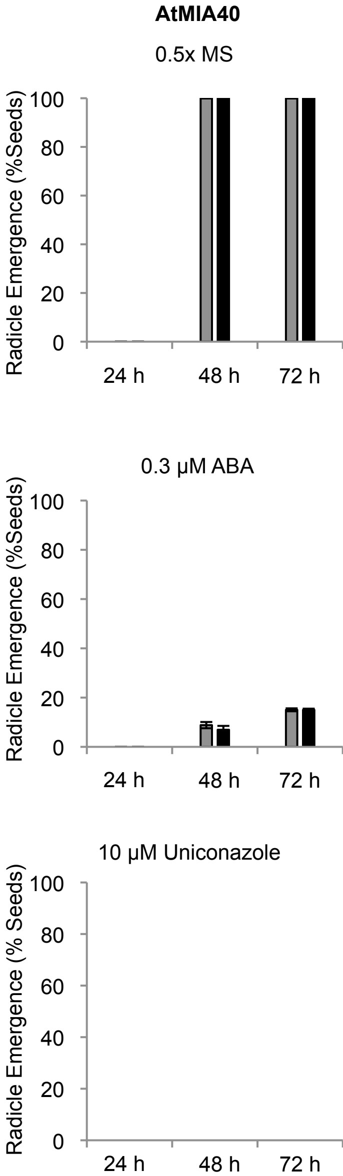

Supplemental Figure S12. Quantitative measurement of seed germination on 0.5 x MS-agar plates containing ABA or Uniconazole. Control plates consisted of 0.5 x MS only. Germination of *atmia40* (grey; left) and WT Col-0 (black; right) seeds is shown. Seed germination was equal across all seed types and conditions. All seeds were imbibed at 4°C for 48 h on each plate prior to germination under 16 h light: 8 h dark at 23°C. Error bars represent ± standard error (n=3 plates of 100-150 seeds each).